Photocatalytic degradation of methylparaben by TiO_2: Multivariable experimental design and mechanism

Yixin Lin [a,b,*], Corinne Ferronato [b], Nansheng Deng [a], Feng Wu [a], Jean-Marc Chovelon [b]

[a] School of Resources and Environmental Science, Wuhan University, Wuhan 430079, PR China
[b] Université Lyon 1, UMR CNRS 5256, Institut de recherches sur la catalyse et l'environnement de Lyon (IRCELYON), 2 Avenue Albert Einstein, F-69626 Villeurbanne, France

ARTICLE INFO

ABSTRACT

Methylparaben is widely used as a bactericide and as an antimicrobial agent in the formulation of personal care products (PCPs) such as tooth pastes, deodorants, beauty creams, solar filters, and bath gels. Owing to a certain estrogenic activity, a possible relationship with breast cancer has been proved by many researchers. Photocatalytic degradation of methylparaben was carried out in an aqueous suspension of TiO_2 irradiated by ultraviolet light. A multivariable center composite design based on response surface methodology was applied to estimate the individual and interaction factors including pH, TiO_2 loading, oxygen concentration and light flux. An acceptable semi-empirical expression ($R^2 = 0.9896$) was obtained via data analysis to predict the response of 50% methylparaben removal time, and optimal experimental conditions were also achieved thanks to the experimental design (pH 9, TiO_2 loading 2.5 g L^{-1}, dissolved oxygen concentration 18 mg L^{-1} and light flux 5.8×10^{15} photo- photons s^{-1} cm^{-2}). Under these conditions, after 6 h of irradiation, 80% of methylparaben miner- alization evaluated through total organic carbon measurement was obtained and 10 photocatalytic intermediates were identified by GC–MS. In addition, a tentative reaction pathway was proposed.

© 2008 Elsevier B.V. All rights reserved.

1. Introduction

Preservatives and/or antimicrobial agents are commonly used in personal care products and pharmaceuticals (PPCP) [1–3]. These compounds are rapidly being detected at ever increasing concentrations: (1) environmentally in ground water and soil; and (2) in human blood, breast milk and tissue [4,5] leading to growing public concern over the possible impact on human health [6,7].

Parabens, alkyl and aryl esters of p-hydroxybenzoic acid, are compounds with bactericide and antimicrobial properties employed mainly in the formulation of personal care products (PCPs) such as tooth pastes, deodorants, beauty creams, solar filters, and bath gels. In addition, they are added to canned foods and beverages as preservatives and less often to textiles [8–10]. Like many personal care chemicals, they are continuously released into aquatic media through domestic wastewater. Therefore, a growing concern has arisen in relation to their potential long-term effects on wildlife and human beings. Lately, in vivo studies have proven that parabens show a certain estrogenic activity [11–13], and ng L^{-1} level concentrations of especially methylparaben and propylparaben have been detected in river water samples [14]. Moreover, in recent studies, a possible relationship between breast cancer and prolonged dermal expositions to paraben containing products has been shown [15] and these have therefore been classified as emerging environmental pollutants by the U.S. Environmental Protection Agency.

Among advanced oxidation processes (AOPs), UV irradiation and titanium dioxide (TiO_2) photocatalysis are gaining growing acceptance as effective wastewater treatment methods. Under UV irradiation, electrons were released from the semiconductor valence band. Photogenerated electrons and holes react with water, dissolved oxygen and organic pollutants to form radicals, forcing a strong oxidation environment. This process can be carried out under ambient conditions (atmospheric oxygen is used as the oxidant) and may lead to complete mineralization of organic carbon into CO_2. Moreover, TiO_2 photocatalyst is widely available, inexpensive, non-toxic and demonstrates relatively high chemical stability. The utilization of combined photocata- lysis and solar technologies may be developed as a useful process for the reduction of water pollution by pollutant compounds because of the mild conditions required and their efficiency in the mineralization [16–18].

* Corresponding author at: Institut de recherches sur la catalyse et l'environne- ment de Lyon (IRCELYON), UMR CNRS 5256, 2 Avenue Albert Einstein, F-69626 Villeurbanne, France. Tel.: +33 4 72 43 26 38; fax: +33 4 72 44 84 38.
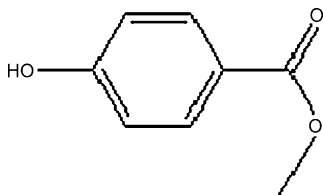E-mail address: yixin.lin@ircelyon.univ-lyon1.fr (Y. Lin).

Fig. 1. Chemical structure of methylparaben.

Various parameters, such as initial analyte concentration, pH values, TiO$_2$ loading, light flux, dissolved oxygen concentration, temperature, as well as photoreactor dimensions, can influence the kinetics of degradation performed by heterogeneous photocatalysis. Most research focuses on investigating the effects of these parameters on the photocatalysis individually. In this case, only one parameter is varied at a time so as to study its influence while other parameters theoretically remain constant. However, this may only be a partial approach of exploring these parameters experimentally since it ignores possible interactions between them. An alternative method, experimental statistical design, can overcome this shortcoming. Recently, the multivariable analysis method has been applied to investigate the operational parameter for dyes and PCPs during photocatalysis [19–21].

In this paper, degradation by methylparaben photocatalysis (see structure, Fig. 1) was studied using the chemometric approach based on a surface response methodology. Important parameters, such as pH values, TiO$_2$ loading, dissolved oxygen concentration, light flux, were investigated in the experimental design. The identification of possible major photoproducts and evaluation of the rate of the mineralization were also investigated.

2. Materials and methods

2.1. Materials and reagents

Analytically pure methylparaben was purchased from Aldrich (St. Quentin-Fallavier, France) and has been used as received. Non-porous titanium dioxide (TiO$_2$, P25, Degussa AG, Germany) with primary particle diameter of 30 nm, specific surface area of 50 m^2 g^{-1}, and crystal distribution of 80% anatase and 20% rutile was used as the photocatalyst directly without pretreatment. Polyvinylidene fluoride (PVDF, i.e. [–(CH$_2$–CF$_2$)$_n$–]) filters (0.45 μm) were purchased from Millipore (Bedford, USA). HPLC grade methanol was purchased from SDS (Peypin, France). Ultrapure water was obtained from a Millipore Waters Milli-Q water purification system. Other reagents were at least of analytical grade.

2.2. Photoreactor and light source

The experiments were carried out in an open Pyrex glass cell (4.0 cm diameter, 15 cm height) located above the light source. The light source was a Philips HPK 125 W mercury high pressure UV lamp with main emission wavelength in the near UV (mainly around 365 nm). IR radiation was filtered out by water circulating in the reactor jacket thermostatic at 20 °C. A Corning 0–52 light filter was used to avoid direct photolysis by UV irradiation below 340 nm. To adjust the intensity of the light source, various types of mesh screen made of stainless steel were adapted between the lamp and the reactor. The actual light flux entering the reactor was measured directly using uranyl oxalate as an actinometer.

2.3. Experimental procedure

Methylparaben stock solution (100 mg L^{-1}) was prepared using Milipore Milli-Q deionized water and stored at 4 °C in the dark. For degradation experiments, the solutions were diluted from the stock solution into the desired concentration (10 mg L^{-1}) and irradiated to study the degradation and the effects of several parameters on the degradation rate. The stock solution was used directly without dilution in order to be able to identify intermediates.

The pH values (3, 6, or 9) were adjusted by adding concentrated aqueous solutions of HCl or NaOH to the desired value throughout the experiments. A magnetic stirrer was used to induce satisfactory mixing of the solution in the reactor. Oxygen gas was bubbled into the reaction suspension to enhance dissolved oxygen concentration up to 18 mg L^{-1}. Under anoxic condition, the suspension was continuously purged with nitrogen gas. The oxygen concentrations were measured by Dissolved Oxygen Pocket meter Oxi 315i (Wissenschaftlich-Technische Werkstätten, Germany).

A volume of 25 mL of aqueous methylparaben solution was introduced into the reactor and the required amount of TiO$_2$ powder was added according to the experimental design (0.5, 1.5 or 2.5 g L^{-1}). The height of a 25 mL suspension in the reactor was about 2 cm. Before irradiation, the suspension was stirred in the dark for 30 min to reach adsorption–desorption equilibrium. For degradation experiments, during the irradiation, aliquots suspension were sampled at regular time intervals and filtered through 0.45 μm PVDF syringe filters to remove TiO$_2$ particles immediately before analysis. Total volume of the sample withdrawn was less than 10% (by volume) of the suspension (i.e. 2.5 mL).

2.4. Analytical procedures

2.4.1. High performance liquid chromatography–diode array detector

The concentration profile of methylparaben during irradiation was analyzed using Shimadzu VP series HPLC system consisting of a LC-10AT binary pump, a SPD-M10A DAD and Shimadzu Class-VP software (Version 5.0). Analytical separation was performed by Yperspher BDS C18 column (particle size 5 μm, 125 mm length × 4.0 mm i.d.). The mobile phase was a mixture of water and methanol, with a ratio of 35% methanol at a flow rate of 1.0 mL min^{-1}. The detection wavelength was 254 nm and injection volume 20 μL.

2.4.2. Solid-phase extraction

Before separating and identifying the intermediates formed during the methylparaben photocatalytic degradation, the filtered suspensions were concentrated by solid-phase extraction (SPE) method. The filtered suspensions at different irradiant time intervals were extracted using 6 mL cartridges packed with 200 mg ENV$^+$ (International Sorbent Technology Ltd., UK). The cartridges were conditioned with 10 mL methanol followed by 10 mL acidified water (pH 2) at a flow rate of 2 mL min^{-1} using a Varian vacuum manifold. Subsequently, 25 mL sample were passed through the cartridge at a flow rate of 2 mL min^{-1}. The analyses were eluted using two aliquots of 1 mL methanol at a flow rate of 2 mL min^{-1}.

2.4.3. Gas chromatography–mass spectrometry

Methylparaben and its intermediates or photoproducts were determined using GC–MS. The system was a PerkinElmer Clarus 500 system consisting gas chromatography connected to a quadrupole spectrometer (PerkinElmer Clarus 500). Separations were carried out using an Elite 5 MS capillary column (5% diphenyl–95% dimethylsiloxane) of 60 m length, 0.25 mm internal diameter and 1.0 μm film thickness. Helium was used as the carrier gas at a constant flow of 1.6 mL min^{-1}. The oven temperature was programmed as follows: 50 °C maintained for 3 min, ramped at 5 °C min^{-1} to 260 °C (maintained for 20 min). The GC–MS interface

and source temperatures were both set at 250 °C. The temperature of the injector was maintained at 250 °C and injections of 1 μL were made in the split mode. The mass spectrometer was operated in electron impact (EI) mode with a potential of 70 eV and the spectra were recorded in a scan range from 33 to 550 m/z with a scan time of 0.3 s and interscan of 0.01 s. Electron impact mass spectra were identified using the NIST 2002 Library and most of these compounds were automatically identified by the NIST MS-Search software.

2.4.4. Total organic carbon analysis

To determine the extent of mineralization during photocatalysis, total organic carbon of filtered suspension samples were measured via a Shimadzu TOC-V$_{CSH}$ analyzer equipped with a Shimadzu ASI-V auto sampler device. One millilitre sample was mixed with 5% HCl solution (2N) by purging out air for 90 s. Each sample was detected twice and a final TOC value was determined by calculating the average over the two measurements. Calibration was achieved by injecting standards of succinic acid solution.

2.4.5. Experimental design data analysis

The chemometric approach was performed using a central composite design (CCD). Analysis of the experimental data was supported by the statistical graphics software system STAT-GRAPHICS Centurion Version XV (STSC, Rockville, USA).

3. Results and discussion

3.1. Preliminary experiments

Methylparaben is resistant to hydrolysis in hot and cold water [22]. Before carrying out experimental design, it is necessary to study the extent of adsorption and photolysis processes on methylparaben. Fig. 2 shows the kinetic profile of methylparaben concentration (C/C_0) under three different conditions: (1) in the dark with TiO$_2$ (adsorption); (2) UV irradiation without TiO$_2$ (photolysis); (3) UV irradiation with TiO$_2$ (photocatalysis). As can be seen, the methylparaben concentration decreased by less than 5% after 120 min irradiation in the absence of TiO$_2$ showing no obvious photolysis. With TiO$_2$ alone without UV irradiation, loss of methylparaben in solution was not evident, indicating insignificant adsorption of methylparaben onto TiO$_2$. It also suggests that stereochemical configuration of methylparaben is inadapted to chelate with TiO$_2$, leading to negligible chemical adsorption of

methylparaben onto the TiO$_2$ surface (a negligible adsorption was also observed at pH 9, which is near to the pK_a of methylparaben, result not shown here). However, in the presence of TiO$_2$ with UV radiation, much faster degradation of methylparaben occurred compared to the reaction either without TiO$_2$ or with only irradiation. Comparing the kinetics of photolysis, adsorption and photocatalysis, this indicates that the methylparaben photocatalysis experiments were carried out at a nearly pure photocatalytic condition with negligible photolysis and adsorption.

3.2. Degradation kinetics

Many experimental results indicated that the photocatalysis degradation rate of various organic chemicals by TiO$_2$ followed the Langmuir–Hinshelwood kinetics model in which Eq. (1):

$$r = -\frac{dC}{dt} = k_{LH}\theta = k_{LH}\frac{K_L C_{eq}}{1 + K_L C_{eq}} \tag{1}$$

where r is the reaction rate of the reactant, which varies proportionally with the coverage θ, k_{LH} is the apparent L–H rate constant for the reaction, K_L is the Langmuir adsorption constant and C_{eq} is the concentration at adsorption equilibrium. At low concentration, $K_L C_{eq}$ can be neglected with respect to 1 ($K_L C_{eq} \ll 1$) and one can get the simplified expression:

$$r = -\frac{dC}{dt} = k_{LH} K_L C_{eq} = k_{app} C_{eq} \tag{2}$$

and hence

$$\ln\frac{C_{eq}}{C} = k_{app}t + \text{constant} \tag{3}$$

Fig. 3 shows the process profile of methylparaben photocatalysis by TiO$_2$ during irradiation. In recent publications, Ollis [23] and Emeline et al. [24] have shown that a pseudo-steady state analysis could be applied instead of the L–H model. However, according to Fig. 3, our data are consistent with the Langmuir–Hinshelwood model since by plotting $\ln(C_{eq}/C)$ versus time, a straight line is obtained, the slope of which upon linear regression equals the apparent pseudo-first-order rate constant $k_{app} - 1$st-order kinetics ($r = k_{app}C_{eq}$, $k_{app} = 0.01809$ min^{-1}), with a good correlation ($R^2 = 0.99732$).
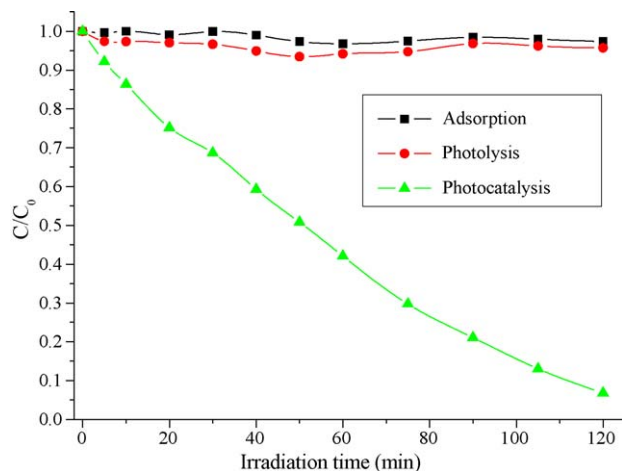

Fig. 2. Comparison of photolysis, adsorption and photocatalysis kinetics of methylparaben: [TiO$_2$] = 2 g L^{-1}, [MP] = 10 mg L^{-1}, pH 6.0, $\Phi = 5.8 \times 10^{15}$ photons s^{-1} cm^{-2}, and [O$_2$] = 9 mg L^{-1}.
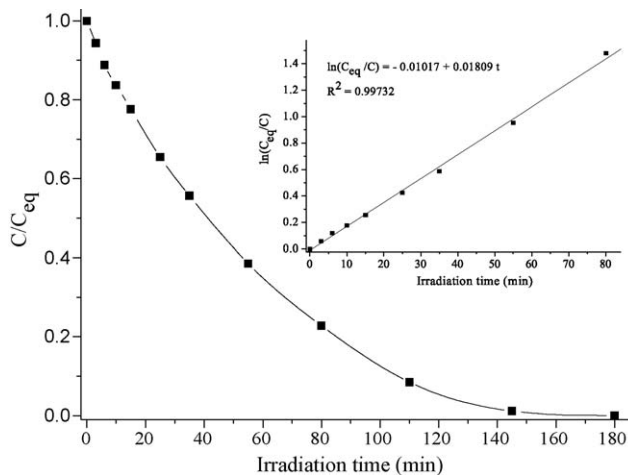

Fig. 3. Kinetic profile of methylparaben photocatalysis: [MP] = 10 mg L^{-1}, [TiO$_2$] = 2 g L^{-1}, pH 9, $\Phi = 5.8 \times 10^{15}$ photons s^{-1} cm^{-2}, and [O$_2$] = 18 mg L^{-1}.

3.3. Experimental design

3.3.1. Choosing factors and response

It has been demonstrated that catalyst dosage, character and initial concentration of the target compound, UV light intensity, oxygen concentration, temperature, and pH for aqueous phase photoreactions are the main parameters affecting the degradation rate. However, it is quite difficult to carry out an experimental design including all these factors because of the large number of experiments and complex data analysis required. Therefore, the more important factors were chosen in the preliminary experimental part. It was found that the four factors, TiO_2 loading, pH, light intensity and oxygen concentration, have the most significant effect on methylparaben photocatalysis rate. This means that all the experiments were carried out at constant temperature (20 °C) and initial methylparaben concentration of 10 mg L^{-1} in the central composite design. In addition, the irradiation time of 50% methylparaben photocatalytic degradation (half-time) was chosen as the response factor.

3.3.2. Central composite design

A response surface methodology based on the central composite design was used to determine the optimum conditions for photocatalytic degradation methylparaben by TiO_2 and to optimize the methylparaben degradation time. Using codified values of the variables, such as pH, TiO_2 loading, oxygen concentration and light intensity, it is possible to obtain a polynomial expression that semi-empirically describes the response. Table 1 summarizes the three levels for each factor involved in the design.

The central composite design consisted of 28 experiments divided into three blocks: (a) four variables ($n = 4$) at two levels: low (-1) and high ($+1$), full factorial design 2^4 (all possible combinations of codified values $+1$ and -1); (b) 8 ($2n$) axial points located at the center and both extreme levels; (c) 4 central replicates of the central points, as shown in Table 2. It also shows actual experimental results (Y_{exp}) and data obtained from the center composite design (Y_{calc}) for the response (Y) corresponding to removal time of 50% methylparaben (half-time).

A semi-empirical expression in Eq. (4) consisting of 17 statistically significant coefficients was obtained from the data analysis using the statistical graphics software STATGRAPHICS Centurion Version XV at 95% confidence level ($p < 0.05$).

$$Y = 2777.3 - 124.8X_A - 71.3X_B - 89.8X_C - 812.3X_D$$
$$+ 21.9X_AX_B + 2.8X_AX_C + 20.3X_AX_D + 37.4X_B{}^2$$
$$+ 17.6X_BX_C + 181.2X_BX_D + 24.8X_CX_D + 64.3X_D{}^2$$
$$- 3.6X_AX_BX_D - 0.5X_AX_CX_D - 2.9X_BX_CX_D - 14.2X_BX_D{}^2$$
$$- 1.7X_CX_D{}^2 \tag{4}$$

where X_A = pH, X_B = [TiO_2], X_C = [O_2], and X_D = light flux.

The experimental design was modeled by Eq. (4) ($R^2 = 0.9896$). It can be improved by comparing the actual experimental data (Y_{exp}) with data predicted by the (Y_{calc}) model as shown in Table 2. It can also be confirmed by model validation (Section 3.6).

Table 1
Range of the parameter variation used in the central composite design.

Parameter	Notation	Low level (-1)	Center level (0)	High level ($+1$)
X_A	pH	3	6	9
X_B	[TiO_2] (g L^{-1})	0.5	1.5	2.5
X_C	[O_2] (mg L^{-1})	0	9	18
X_D	Φ ($\times 10^{15}$ photons s^{-1} cm^{-2})	1.2	3.5	5.8

Table 2
Experimental data in central composite design.

No.	Pattern	Block	pH	[TiO$_2$]	[O$_2$]	Φ	Y_{exp} (min)	Y_{calc} (min)	Comment
1	$-1 -1 -1 -1$	a	3	0.5	0	1.2	1382	1372	Full factorial
2	$+1 -1 -1 -1$		9	0.5	0	1.2	829	821	Full factorial
3	$-1 +1 -1 -1$		3	2.5	0	1.2	683	670	Full factorial
4	$+1 +1 -1 -1$		9	2.5	0	1.2	334	329	Full factorial
5	$-1 -1 +1 -1$		3	0.5	18	1.2	505	497	Full factorial
6	$+1 -1 +1 -1$		9	0.5	18	1.2	198	190	Full factorial
7	$-1 +1 +1 -1$		3	2.5	18	1.2	310	303	Full factorial
8	$+1 +1 +1 -1$		9	2.5	18	1.2	212	206	Full factorial
9	$-1 -1 -1 +1$		3	0.5	0	5.8	157	150	Full factorial
10	$+1 -1 -1 +1$		9	0.5	0	5.8	106	110	Full factorial
11	$-1 +1 -1 +1$		3	2.5	0	5.8	97	102	Full factorial
12	$+1 +1 -1 +1$		9	2.5	0	5.8	74	71	Full factorial
13	$-1 -1 +1 +1$		3	0.5	18	5.8	95	97	Full factorial
14	$+1 -1 +1 +1$		9	0.5	18	5.8	59	62	Full factorial
15	$-1 +1 +1 +1$		3	2.5	18	5.8	70	70	Full factorial
16	$+1 +1 +1 +1$		9	2.5	18	5.8	40	42	Full factorial
17	$-1 0 0 0$	b	3	1.5	9	3.5	214	223	Axial
18	$+1 0 0 0$		9	1.5	9	3.5	135	142	Axial
19	$0 -1 0 0$		6	0.5	9	3.5	182	191	Axial
20	$0 +1 0 0$		6	2.5	9	3.5	144	153	Axial
21	$0 0 -1 0$		6	1.5	0	3.5	194	188	Axial
22	$0 0 +1 0$		6	1.5	18	3.5	85	81	Axial
23	$0 0 0 -1$		6	1.5	9	1.2	303	311	Axial
24	$0 0 0 +1$		6	1.5	9	5.8	48	50	Axial
25	$0 0 0 0$	c	6	1.5	9	3.5	129	134	Center
26	$0 0 0 0$		6	1.5	9	3.5	129	134	Center
27	$0 0 0 0$		6	1.5	9	3.5	129	134	Center
28	$0 0 0 0$		6	1.5	9	3.5	129	134	Center

3.3.3. Standardized Pareto chart

To visualize the importance of the calculated factors in Eq. (4), Fig. 4 presents the single factor and interaction factors depicted in rank order in the form of Pareto chart. All the standardized factors were in the absolute values and surpass the vertical significance line (95% confidence intervals) which exerts a statistically significant influence on the response. The signs + and − represent positive and negative effects, respectively. Positive effect indicates that degradation half time increases in the presence of high levels of the respective variables within the range studied; while negative effect indicates that degradation half time increases in the presence of low levels. Positive quadratic or third order polynomial coefficients indicate a synergistic effect, while negative coefficients, an antagonistic effect between or among the variables.

As Fig. 4 shows, for individual factors, the most important parameter for methylparaben photocatalysis is light flux (D)
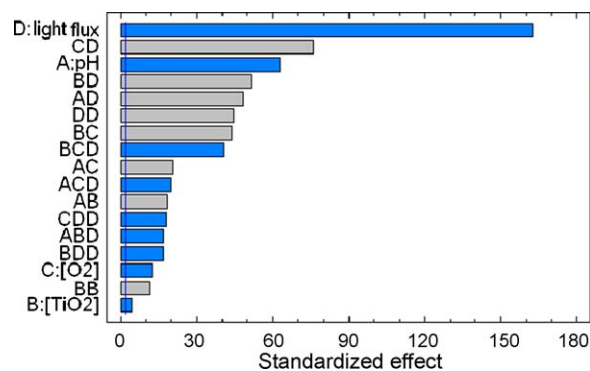

Fig. 4. Standardized effects of single and interaction factors on the degradation time of 50% methylparaben.
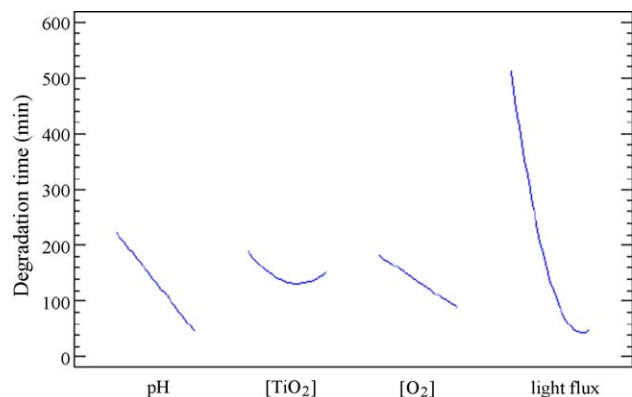
Fig. 5. Graphical presentation of the statistical evaluation of the effects of individual factors on the methylparaben photocatalysis.

followed by pH value (*A*) whereas oxygen concentration (*C*) and TiO$_2$ loading (*B*) have less importance among the four single parameters based on 95% significance. On the other hand, the methylparaben photocatalysis is affected by quadratic (DD, BB), two-way interactions (CD, BD, AD, BC, AC, and AB) and even third-order polynomial factors (BCD, ACD, CDD, ABD, and BDD).
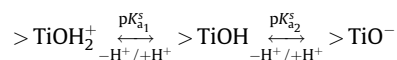
3.4. Main effect plots

The influence of all the single factors considered is depicted in Fig. 5 wherein the lines indicate the estimated change in response (50% removal time) as each factor is moved from its low level to its high level, while maintaining all other factors constant at a midway value codified as value 0, between their low and high values.

3.4.1. pH Value

In the wide range of 3–9, pH markedly influences the efficiency of the photocatalytical processes of methylparaben at not only first order but also at quadratic level, which agrees with many research works [25–27]. The pH dependence can be associated with changes of the surface charge of the photocatalyst, net charge of pollutant and amount of HO$^\bullet$ produced. This can lead to a modification of the overall rate. Additionally, changes in pH may introduce deactivation problems if the presence of long-living intermediates that poison the photocatalyst is favored [28].

The interaction of electron donors and acceptors with metal oxide semiconductors is determined in part by surface chemistry. In the case of TiO$_2$, the principal amphoteric surface functionality is the "titanol" moiety, >TiOH. Hydroxyl groups on the TiO$_2$ surface are known to take part in the following acid–base equilibrium [29]:

$$> \text{TiOH}_2^+ \underset{-\text{H}^+/+\text{H}^+}{\overset{\text{p}K_{a_1}^s}{\longleftrightarrow}} > \text{TiOH} \underset{-\text{H}^+/+\text{H}^+}{\overset{\text{p}K_{a_2}^s}{\longleftrightarrow}} > \text{TiO}^-$$

where p$K_{a_1}^s$ and p$K_{a_2}^s$ represent the negative log of microscopic acidity constants of the first and second acid dissociation, respectively. For Degussa P25, the pH of point of zero charge, pH$_{pzc}$, is 6.25 [30]. This implies, that cationic electron acceptors will be favored at pH > pH$_{pzc}$ conditions, while anionic electron donors will be favored at pH < pH$_{pzc}$ conditions. The ionization state of the TiO$_2$ surface at high pH value is beneficial to methylparaben photocatalysis, which is clearly shown in Fig. 5. Therefore, the interaction relationship between pH and TiO$_2$ (AB) indicated in Fig. 4 is an important interaction factor even if it is weaker.

The state of methylparaben in aquatic solution is also affected by the pH, closely related with its dissociation constant. When the pH is lower than the pK_a of the methylparaben (pK_a = 8.3), it is primarily present in the molecular state. In contrast, it exists in ionic form if pH > pK_a. But relating the dissociation constant of chemical to its interaction with the catalyst surface is only a rough approximation because this value is in principle valid only for bulk liquids. The formation of a double layer at the liquid–solid interface can influence both the dissociation and the polarizability of reacting molecules [31]. Therefore, the photocatalysis becomes more efficient at alkaline pH range, above the pK_a of methylparaben.

The pH value may also influence the amount of hydroxyl radicals (HO$^\bullet$) formed. HO$^\bullet$ can be formed by the reaction between hydroxide ions and light-excited holes (h$^+$) with H$_2$O/HO$^\bullet$. The positive holes are considered as the major oxidation species at low pH whereas hydroxyl radicals are considered as the predominant species at neutral or high pH levels [32,33]. As shown in Fig. 5, the degradation time decreases obviously from acid pH 3 to alkaline pH 9. This indicates that in alkaline solution $^\bullet$OH are more easily generated by oxidizing more hydroxide ions available on TiO$_2$ surface, thus the efficiency of the process is logically enhanced.

3.4.2. Light flux

The light flux is the most important factor among all the factors considered from first order to third order ones, as shown in Fig. 4. This is consistent with previous works carried out in our laboratory [21]. As shown in Fig. 5, there are two photocatalytic degradation regimes with respect to the UV light flux in the range studied: (i) at low light intensities (1.2 × 10^{15} photons s^{-1} cm^{-2} < Φ < 4.0 × 10^{15} photons s^{-1} cm^{-2}), the half-life decreases linearly with increasing light intensity (first order), which means the photons are converted into active species to take part in the photocatalytic degradation immediately [34] and (ii) at intermediate light intensities beyond a certain value (4.0 × 10^{15} photons s^{-1} cm^{-2} < Φ < 5.8 × 10^{15} photons s^{-1} cm^{-2}), the rate varied as functional order between zero and one. In the former regime, the electron–hole pairs are consumed more rapidly by chemical reactions than by recombination reactions, whereas in the latter regime, the recombination rate is dominant [35–37]. The significant quadratic effect (DD) (see Fig. 4) is the main reason for primary electron–hole recombination at higher light intensities range.

It should be pointed out that a very important interaction effect exists between the two most important factors, pH and light flux (see Fig. 4, AD). This synergistic interaction effect denotes a positive interdependence of photocatalytic rate on pH and light flux. With a higher pH value and stronger light intensity, the reaction can attain a faster degradation rate. Moreover, at high pH value, increasing light flux promotes much more positive influence on methylparaben degradation time than that at low pH value.

3.4.3. Oxygen concentration

As Fig. 4 shown, oxygen concentration is an essential factor of methylparaben photocatalytic degradation, even if less important, which is consistent with many research works [38,39]. It is confirmed in Fig. 5 that oxygen concentration has a positive effect on the degradation process. The removal time decreases linearly with the increase of dissolved oxygen concentration. Reductive transformation of methylparaben, which can occur under certain experimental conditions (oxygen absence and purging nitrogen gas), is usually much less efficient than the oxidative one due to two reasons. Firstly, the reducing power of a conduction band electron is significantly lower than the oxidizing power of a valence band hole. Secondly, most reducible substrates do not compete kinetically with oxygen in trapping photogenerated conduction band electrons [40].

Dissolved molecular oxygen is strongly electrophilic and thus an increase of its content probably reduces unfavorable electron–hole recombination routes [35,41], so it is reasonable that it can attain less removal time at higher oxygen concentration. But higher concentrations lead to a downturn of the reaction rate, which could be attributed to the fact that the TiO_2 surface becomes highly oxygenated to the extent of inhibiting the adsorption of pollutant at active sites [42]. This relationship between oxygen concentration and TiO_2 loading is significant and indicated by an interaction factor BC in Fig. 4. Generally, it is assumed that O_2 gas adsorbs onto TiO_2 from the liquid phase, where oxygen concentration is proportional to the gas phase pressure of O_2 according to Henry's law. So the dissolved oxygen plays a key role in the degradation of methylparaben, apart from its conventional electron scavenging function [43].

It is worth noticing that there is a quite significant interaction factor between oxygen and light flux (see Fig. 4, CD). This positive interaction factor indicates that the methylparaben photocatalytic process may require much less removal time at higher oxygen concentration and stronger light flux. At high oxygen concentration, the reaction rate increases with increasing light intensity linearly or half-order [31], since more $HO^\bullet$ forms with boosting light flux. The positive interaction factor between pH and oxygen concentration (see Fig. 4, AC) is another significant factor in the experimental design. pH value also influences the amount of $HO^\bullet$ radicals formed by the reaction of light-excited holes with H_2O/$HO^\bullet$. A linear dependence between $HO^\bullet$ formation on TiO_2 surface and O_2 gas pressure was evidenced [44]. The role of oxygen in the ring degradation of some hydroxyl intermediates is very important, especially while some of the hydroxyl aromatics products are potentially more toxic than their parent compounds [45]. Within the range of oxygen concentrations studied ($0–18$ mg L^{-1}), the conversion ratio (or reaction rate) increases with increasing oxygen concentration.

3.4.4. TiO₂ loading

As expected, TiO_2 loading is an important factor with positive effect of the increased number of TiO_2 active sites during photocatalytic degradation. Generally, photocatalytic rate increases with TiO_2 loading increasing due to a higher surface area of TiO_2 that is beneficial to adsorption and degradation. However, as shown in Fig. 5 above a certain concentration of TiO_2 loading, a decrease of the photoreactivity is observed, which is well illustrated by the quadratic factor DD (Fig. 4). Indeed, at higher TiO_2 loading, more of the originally activated TiO_2 may be deactivated through collision with ground-state catalysts according to the following equation:

$$TiO_2^* + TiO_2 \rightarrow TiO_2^\# + TiO_2 \qquad (5)$$

where TiO_2^* are active species adsorbed on its surface and $TiO_2^\#$ is the deactivated form of TiO_2 [46].

On the other hand, at higher TiO_2 loading, agglomeration and sedimentation of TiO_2 can take place, reducing the interfacial area between the reaction solution and the catalyst, and decreasing the number of active sites on the surface. Recent studies [47,48] have shown that agglomeration is highest near the point of zero charge ($pH_{PZC} = 6.25$).

In addition, by considering both TiO_2 loading and light flux, at higher TiO_2 loading, the reaction rate decreases, as shown through the interaction factor BD (Fig. 4) owing to an increase of light scattering on catalyst particles and a decrease of light penetration.

3.5. Contour diagrams and optimal condition

The statistical software can then be used to construct the contour diagram throughout the experimental space after screening
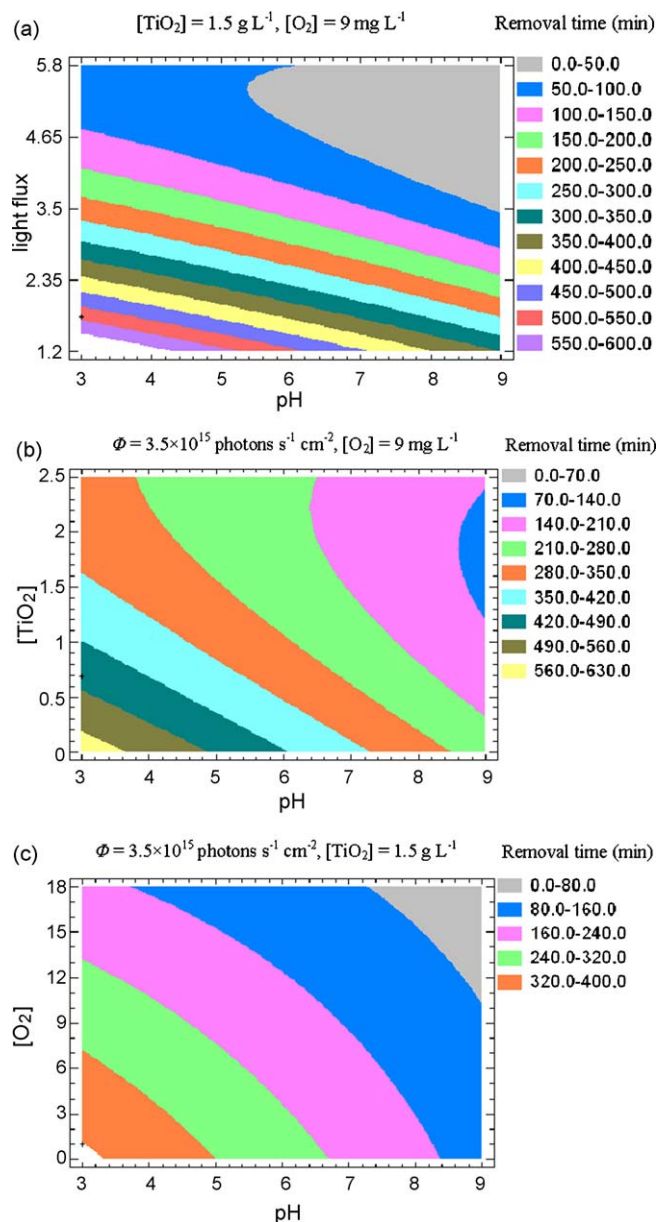

Fig. 6. Contour diagrams of 50% methylparaben removal time: (a) light flux–pH, (b) [TiO₂]–pH, and (c) [O₂]–pH.

out significant single and interaction factors, in order to explore the optimum experimental region for methylparaben photocatalytic degradation. Each contour diagram plot has an infinite number of combinations based on two selected parameters while maintaining the two other factors constant at their middle values.

Table 3
Comparison of predicted and experimental values of the response at optimal region for another three experiments[a].

No.	pH	[TiO₂] (g L⁻¹)	[O₂] (mg L⁻¹)	Φ × 10¹⁵ photons s⁻¹ cm⁻²	Removal time (min) Predicted[b]	Observed[c]
1	7	2.4	18	5.8	45	49
2	7.5	2.2	18	5.8	50	54
3	8	2	18	5.8	42	45

[a] The initial methylparaben concentration is 10 mg L^{-1}.
[b] The values were calculated from semi-empirical expression (Eq. (4)).
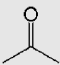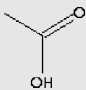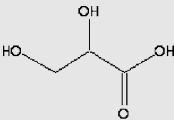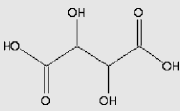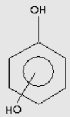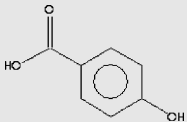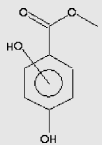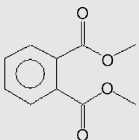[c] Average value on removal time of two experiments at selected condition.
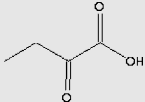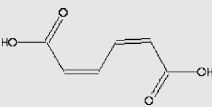
The contour diagrams (Fig. 6), obtained from simulation, show the removal time of 50% methylparaben for the light flux versus pH (Fig. 6a), TiO$_2$ loading versus pH (Fig. 6b) and oxygen concentration versus pH (Fig. 6c), respectively, where the gray regions indicate shorter removal time of response.

As shown in Fig. 6a, the fast removal time can be obtained at high light flux ($\Phi > 3.5 \times 10^{15}$ photons s^{-1} cm^{-2}) and alkaline pH value (7–9). These two factors are the two most important parameters in the experimental design (see Fig. 4). Therefore, the

strong light flux and alkaline pH regions are necessary and important to promote or accelerate methylparaben photocatalysis. As displayed in Fig. 6b, the minimum removal time can be attained at high TiO$_2$ loading in the scope 1.3–2.4 g L^{-1} and high pH value (8–9). As seen in Fig. 6c, the shortest removal time can be achieved at high oxygen concentration within the range of 12–18 mg L^{-1} and at high pH value (7–9). Many investigators have expressed the view [49] that the electron-trapping role of O$_2$ can be the rate and efficiency determining process, so it is important to introduce an

Table 4
Mass spectra data and structures of identified intermediates by GC–MS for irradiation methylparaben with TiO$_2$.

NO.	Structure	Intermediate name	Retention time (min)	Molecular weight (g mol^{-1})	Main fragments (m/z)
1		Acetone	4.3	58	43, 58, 15, 42, 27
2		Acetic acid	4.6	74	43, 45, 60, 15, 42
3		Glyceric acid	5.5	106	75, 47, 45, 43, 74
4		Tartaric acid	8.1	150	76, 58, 29, 70, 31
5		2-Oxobutyric acid	9.2	102	57, 45, 44, 56, 102
6		2,4-Hexadienedioic acid	17.6	142	97, 96, 41, 51, 142
7		Dihydroxybenzene	29.1	110	110, 81, 55, 53, 39
8		4-Hydroxybenzoic acid	34.9	138	121, 138, 93, 65, 39
9		Dihydroxybenzoic acid methyl ester	36.6	168	137, 168, 81, 109, 59
10		1,2-Benzenedicarboxylic acid dimethyl ester	38.1	194	163, 77, 164, 76, 135

aerobic surrounding by introducing oxygen gas for methylparaben photocatalytic degradation.

The optimal experimental condition for the highest photo-catalytic efficiency of methylparaben estimated by multivariable experimental design is as follows: light flux: 5.8×10^{15} photo-photons s^{-1} cm^{-2}; pH: 9; oxygen concentration: 18 mg L^{-1}; TiO_2 loading: 2.5 g L^{-1}. Compared with univariate approach, the mul-tivariate experimental design is more successful or reasonable to

model the photocatalytic reaction thanks to taking interaction relationship between or among reaction factors into consideration.

3.6. Model validation and confirmation

Verification experiments were carried out at the optimal con-ditions derived from multivariate design, as shown in Table 3. It demonstrates that the experimental values are close to the
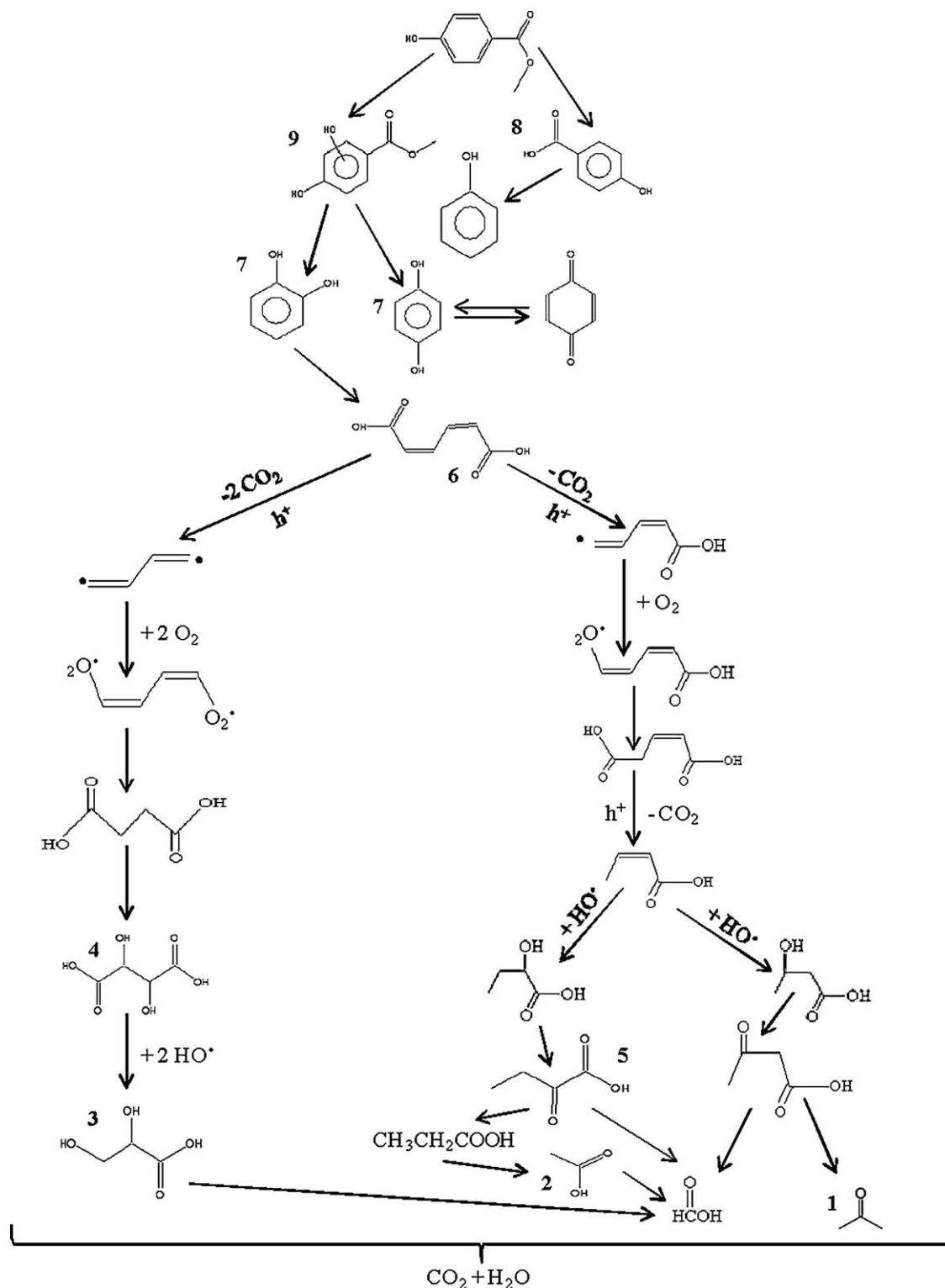

Fig. 7. A tentative mechanism of methylparaben photocatalytic degradation by titanium dioxide.

predicted values from semi-empirical expression (Eq. (4)), which confirms the adequacy and validity of the model for simulating the removal time of methylparaben.

3.7. Photocatalysis intermediates and pathway

The irradiation experiments for the sake of characterizing photocatalytic intermediates were carried out at optimal conditions using stock methylparaben solution (100 mg L^{-1}). The solutions irradiated at different times were analyzed by GC–MS to identify as many intermediates as possible. Ten intermediates were identified as possible degradation products and these are summarized in Table 4 together with their GC–MS retention times, molecular weights, structure and main fragments. Based on the identification results, a tentative reaction pathway of methylparaben oxidation in the presence of illuminated titanium dioxide can be schematically depicted in Fig. 7.

As shown in Fig. 7, all the intermediates are formed in mainly three different ways: (i) HO$^\bullet$ attack on methylparaben molecule, (ii) the reaction of methylparaben molecule with holes photo-generated in titanium dioxide, and (iii) direct oxidation of methylparaben by oxygen dissolved in water. Firstly, methylparaben is attacked by HO$^\bullet$ radicals at –CH$_3$ and –H in the aromatic ring to produce 4-hydroxybenzoic acid (8) and dihydroxybenzoic acid methyl ester (9). It should be pointed out that 1,2-benzenedicarboxylic acid dimethyl ester (10) is also formed because of coupling at high concentration.

These products are further oxidized into the phenol, which is attacked by HO$^\bullet$ radicals to form the isomers of 1, 2-dihydroxybenzene and 1,4-dihydroxybenzene (7). These two aromatic compounds and benzoquinone are well known intermediates of the phenol photocatalytic oxidation [50,51]. Moreover, 1,2-dihydroxybenzene is transformed into 2,4-hexadienedioic acid (6) by the opening of the aromatic ring observed throughout the photocatalysis process, which is also reported in the literature [52,53].

2,4-Hexadienedioic acid (6) is oxidized into many small molecular organic compounds (see Fig. 7) through the following reactions [54]: (i) attack by hydroxy radicals onto methyl, double bond or benzoic ring; (ii) photokolbe reaction which is a decarboxylation of carboxylic acid intermediates via holes; (iii) C=C bond which is attacked firstly by hydroxyl radicals and secondly by O$_2$ to form a peroxide intermediate and then transformed into acid. As can be seen, the pathway that might lead to methyl degradation needs O$_2$. Moreover, the pH values changed from initial pH 9 to pH 5.3, confirming that small molecular weight acid compounds are produced during photocatalysis.

Finally, all the products are possible transformed into carbon dioxide and water lead by the breaking down of the benzene ring and subsequent mineralization, which could be visualized by the decrease in TOC during the photocatalytic process.

3.8. Mineralization

Complete mineralization is very important for organic pollutants photocatalysis. The breaking down of the benzene ring and subsequent mineralization leading to water and carbon dioxide could be visualized by the decrease in TOC during the photocatalytic process. To assess the extent of mineralization during the photocatalytic degradation of methylparaben, TOC was monitored as shown in Fig. 8. It showed TOC decrease during photocatalytic degradation of methylparaben at optimal experimental conditions. Although half the methylparaben was consumed by appropriately 40 min under irradiation under optimal conditions, the corresponding TOC exhibited a slightly decrease,
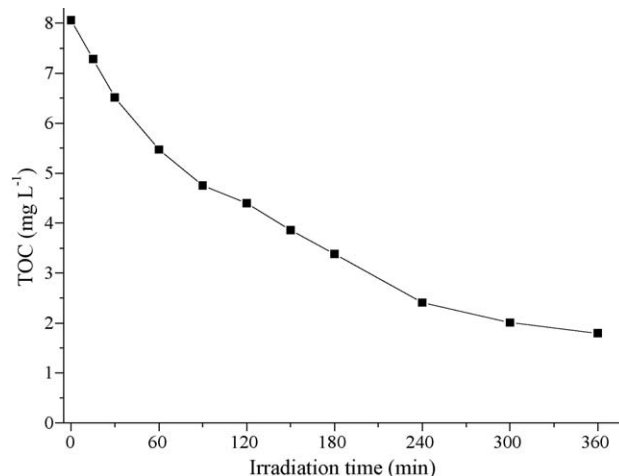

Fig. 8. Total organic carbon (TOC) removal during methylparaben photocatalysis.

indicating that TOC removal followed a much slower rate compared to degradation of methylparaben. However, nearly complete TOC removal (80%) was achieved after long irradiation time (360 min), because of the formation of the more stable intermediates toward photo-oxidation.

4. Conclusions

The photocatalytic degradation of methylparaben has been studied in aqueous solution using TiO$_2$ as photocatalyst and has been proved to be an efficient method of removing methylparaben. pH, TiO$_2$ loading, oxygen concentration and light flux have been systematically evaluated via the center composite design based on response surface methodology. A semi-empirical expression was proposed and successfully used to model the photocatalytic process with high correlation, and an optimal experimental region was also obtained through the contour diagram plots. This multivariable experimental design takes both individual factors and interaction factors into consideration. This is more reasonable and beneficial in investigating the photocatalysis process and predicting its behavior. The identification of intermediates allows us to propose a tentative reaction pathway of methylparaben photocatalysis including attack by HO$^\bullet$ radicals on the alkyl chain, opening of the aromatic ring through hydroxylation to form alkyl carboxylic acid and finally mineralization.

References

[1] H. Cabana, J.H. Jiwan, R. Rozenberg, V. Elisashvili, M. Penninckx, S.N. Agathos, J. Peter Jones, Chemosphere 67 (2007) 770–778.
[2] P.D. Darbre, Best Pract. Res. Clin. Endocrinol. Metab. 20 (2006) 121–143.
[3] M. Lakeram, D.J. Lockley, D.J. Sanders, R. Pendlington, B. Forbes, J. Biomol. Screen. 12 (2007) 84–91.
[4] D.W. Kolpin, M.T. Meyer, M.E. Thurman, S.D. Zaugg, L.B. Barber, H.T. Buxton, Environ. Sci. Technol. 36 (2002) 1202–1211.
[5] J. Heidler, A. Sapkota, R.U. Halden, Environ. Sci. Technol. 40 (2006) 3634–3639.
[6] A.D. Dayan, Int. J. Clin. Pract. 60 (2006) 1009–1013.
[7] C.G. Daughton, T.A. Ternes, Environ. Health Perspect. 107 (Suppl. 6) (1999) 907–938.
[8] M. Borremans, J.V. Loco, P. Roos, L. Goeyens, Chromatographia 59 (2004) 47–53.
[9] Q.L. Zhang, M. Lian, L.J. Liu, H. Cui, Anal. Chim. Acta 537 (2005) 31–39.

[10] S. Doron, M. Friedman, M. Falach, E. Sadovnic, H. Zvia, Int. J. Antimicrob. Agents 18 (2001) 575–578.
[11] P.W. Harvey, D.J. Everett, J. Appl. Toxicol. 24 (2004) 1–4.
[12] T. Benijts, W. Günther, W. Lambert, A.D. Leenheer, Mass Spectrom. 17 (2003) 1866–1872.
[13] D. Pugazhendhi, G.S. Pope, P.D. Darbre, J. Appl. Toxicol. 25 (2005) 301–309.
[14] T. Benijts, W. Lambert, A.D. Leenheer, Anal. Chem. 76 (2004) 704–711.
[15] P.D. Darbre, A. Aljarrah, W.R. Miller, N.G. Coldham, M.J. Sauer, G.S. Pope, J. Appl. Toxicol. 24 (2004) 5–13.
[16] B. Neppolian, H.C. Choi, S. Sakthivel, B. Arabindoo, V. Murugesan, Chemosphere 46 (2002) 1173–1181.
[17] V. Augugliaro, C. Baiocchi, A.B. Prevot, E.G. Lopez, V. Loddo, S. Malato, G. Marci, L. Palmisano, M. Pazzi, E. Pramauro, Chemosphere 49 (2002) 1223–1230.
[18] M. Stylidi, D.I. Kondarides, X.E. Verykios, Appl. Catal. B: Environ. 40 (2003) 271–286.
[19] V.A. Sakkas, P. Calza, C. Medana, A.E. Villioti, C. Baiocchi, E. Pelizzetti, T. Albanis, Appl. Catal. B: Environ. 77 (2007) 135–144.
[20] P. Calza, V.A. Sakkas, C. Medana, C. Baiocchi, A. Dimou, E. Pelizzetti, T. Albanis, Appl. Catal. B: Environ. 67 (2006) 197–205.
[21] M. Sleiman, D. Vildozo, C. Ferronato, J.M. Chovelo, Appl. Catal. B: Environ. 77 (2007) 1–11.
[22] M.G. Soni, S.L. Taylor, N.A. Greenberg, G.A. Burdock, Food Chem. Toxicol. 40 (2002) 1335–1373.
[23] D.F. Ollis, J. Phys. Chem. B 109 (2005) 2439–2444.
[24] A.V. Emeline, V.K. Ryabchuk, N. Serpone, J. Phys. Chem. B 109 (2005) 18515–18521.
[25] R.J. Watts, S. Kong, M.P. Orr, G.C. Miller, B.E. Henry, Water Res. 29 (1995) 95–100.
[26] P. Amézaga-Madrid, G.V. Nevárez-Moorillón, E. Orrantia-Borunda, M. Miki-Yoshida, FEMS Microbiol. Lett. 211 (2002) 183–188.
[27] Y. Koizumi, M. Taya, Biochem. Eng. J. 12 (2002) 107–116.
[28] J. Chen, L. Eberlein, C.H. Langford, J. Photochem. Photobiol. A: Chem. 148 (2002) 183–189.
[29] W. Stumm, Chemistry of Solid–Water Interface, John Wily & Sons, Inc., New York, 1992, 428 pp..
[30] C. Kormann, D.W. Bahnemann, M.R. Hoffmann, Environ. Sci. Technol. 25 (1991) 494–500.
[31] O. Carp, C.L. Huisman, A. Reller, Prog. Solid State Chem. 32 (2004) 33–177.
[32] W.Z. Tang, C.P. Huang, Water Res. 29 (1995) 745–756.
[33] S. Tunesi, M. Anderson, J. Phys. Chem. 95 (1991) 3399–3405.
[34] J.M. Herrmann, Catal. Today 53 (1999) 115–129.
[35] D.F. Ollis, E. Pelizzetti, N. Serpone, Environ. Sci. Technol. 25 (1991) 1522–1529.
[36] K.H. Wang, H.H. Tsai, Y.H. Hseich, Appl. Catal. B: Environ. 17 (1998) 313–320.
[37] M.R. Nimlos, W.R. Jacoby, D.M. Blake, T.A. Milne, Environ. Sci. Technol. 27 (1993) 732–740.
[38] H. Al-Ekabi, A. Safarzadeh-Amiri, W. Sifton, J. Story, Int. J. Environ. Pollut. 1 (1991) 125–130.
[39] F. Mahdavi, T.C. Bruton, Y. Li, J. Org. Chem. 58 (1993) 744–746.
[40] Y. Li, P.V. Kamat, D. Meisel, Semiconductor Nanocluster, Elsevier, Amsterdam, 1993.
[41] S.L. Murov, I. Carmichael, G.L. Huy, Handbook of Photochemistry, Marcel Dekker, New York, 1993.
[42] A.M. Braun, E. Oliveros, Water Sci. Technol. 35 (1997) 17–23.
[43] Y. Wang, C.S. Hong, Water Res. 34 (2000) 2791–12791.
[44] P.F. Schwartz, N.J. Turro, S.H. Bossmann, A.M. Braun, A.M. Abdel-Wahab, H. Dürr, J. Phys. Chem. B 101 (1997) 7127–7134.
[45] J.F. Gierthy, K.F. Arcado, M. Floyd, Chemosphere 34 (1997) 1495–1505.
[46] B. Neppolian, H.C. Choi, S. Sakthivel, B. Arabindoo, V. Murugesan, J. Hazard. Mater. 89 (2002) 303–317.
[47] N. San, M. Kilic, Z. Tuiebakhova, Z. Cinar, J. Adv. Oxide Technol. 10 (2007) 43–50.
[48] C.M. So, M.Y. Cheng, J.C. Yu, P.K. Wong, Chemosphere 46 (2002) 905–912.
[49] J. Cunningham, G.A. Sayyed, P. Sedlak, J. Caffrey, Catal. Today 53 (1999) 145–158.
[50] K. Okamoto, Y. Yamamoto, H. Tanaka, M. Tanaka, A. Itaya, Bull. Chem. Soc. Jpn. 58 (1985) 2015–2022.
[51] V. Augugliaro, L. Palmisano, A. Sclafani, C. Minero, E. Pelizzetti, Toxicol. Environ. Chem. 16 (1998) 89–94.
[52] R. Matthews, J. Catal. 111 (1998) 264–272.
[53] S. Chatterjee, S. Sarkar, S.N. Bhattacharyya, J. Photochem. Photobiol. A: Chem. 81 (1994) 199–203.
[54] M.I. Franch, J.A. Ayllón, J. Peral, X. Domènech, Catal. Today 101 (2005) 245–252.